Geodesy and Geodynamics 2013,4(3):65 -70

http://www.jgg09.com
Doi:10.3724/SP.J.1246.2013.03065

Present-day deformation of Agung volcano, Indonesia, as determined using SBAS-InSAR

Ji Lingyun, Wang Qingliang and Qin Shanlan
Second Crust Monitoring and Application Center, China Earthquake Administration, Xi'an 710054, *China*

Abstract: Based on ALOS PALSAR images, time series deformation fields of the Agung volcano area were obtained using SBAS-InSAR in 2007 -2009. The time series deformation showed obvious inflation around the Agung volcano area, which was positively correlated with time. We modeled the cumulated deformation interferogram based on Mogi point source and vertical prolate spheroid source. The deformation model indicated that the vertical prolate spheroid model fit the observed deformation reasonably well. The magma chamber was located beneath the center of the volcano at a depth of approximately 5 km beneath the summit.
Key words: SBAS-InSAR; time series deformation; magma chamber parameter; atmospheric phase screen; volcanic activity

1 Introduction

Agung is a stratovolcano located on the eastern side of Bali Island, Indonesia, and possesses a summit elevation of 3142 meters (Fig. 1). The volcano lies 300 km north of the Java trench, where the Indo-Australian plate subducts beneath southeast Asia. Agung presents the highest peak on Bali Island. The volcano's cone is steep and is almost barren on top, possessing an open funnel-shaped crater measuring 520 × 375 meters[1]. Over the past 200 years, Agung has erupted several times, including in 1808, 1821, 1843, 1963-64. The tremendous explosive eruption in 1963, which was classified as a Plinian eruption, claimed more than 1000 lives, and the dust cloud spread over the entire globe[2]. Due to these contemporary eruptions, it is necessary to determine whether Agung is still active. However, ground-based monitoring has not been performed in the Agung volcano area until now due to socioeconomic and logistical barriers, which makes the application of satellite-based monitoring techniques such as satellite-based synthetic aperture radar interferometry (InSAR) highly desirable. InSAR combines two SAR images taken at different times from nearly the same point in space to determine the deformation of the area along the radar's line of sight (LOS) over time.

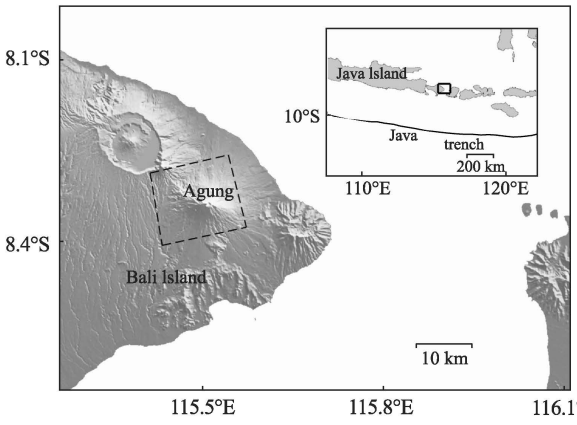

Figure 1 Shaded relief topographic map of the area surrounding the Agung volcano in eastern Bali Island. The inset shows the location of Bali Island (small rectangle) and the surrounding area. The dashed-line box outlines the interferogram area. The heavy solid line in the inset maps the Java trench

Received:2013-02-06; Accepted:2013-03-04
Corresponding author: Ji Lingyun, Tel: +86-29-85506715, E-mail: dinsar010@163.com
This work was supported by the Special Earthquake Research Project, China Earthquake Administration (201208009).

In the past two decades, InSAR has been proved to be a useful tool for surveying large regions of deformation in volcanic areas[3-6]. Currently, SBAS-InSAR (Small Baseline Subsets, Interferometric Synthetic Aperture Radar) is widely used in detecting volcanic deformation[7-11] for it could reduce decorrelation. In the present study, we used SBAS-InSAR to detect potential deformation fields in 2007 - 2009. To understand the physical development of the volcanic system during this time period, we used a Mogi source model and a vertical prolate spheroid model to inverse the parameters of the magma chamber.

2 Data and method

2.1 SAR data and analysis

Due to the presence of dense vegetation cover, we used ALOS PALSAR data, which operates on the L band and is less susceptible to vegetation. Between January of 2007 and January of 2009, ALOS acquired 14 radar images covering the Agung volcano region and provided 2 years of continuous observations.

Our goal was to detect any possible deformations; thus, the most efficient strategy was to make interferograms spanning long time periods so that the magnitude of the deformation was as high as possible. However, this approach failed for the Agung volcano area due to temporal decorrelation, which was caused by densely covered forest. Even though L-band SAR images were selected, interferograms spanning time intervals of 6 months or longer typically possessed large decorrelated areas. Even at intervals of less than 6 months, the western flank of the volcano was decorrelated in many interferograms, but coherence on the northeastern flank was good. Longer perpendicular baselines can be used to increase the percentage of decorrelation, but only at the shortest time intervals, and perpendicular baseline values up to 800 m usually produce good results[12].

2.2 Method of InSAR data processing

Traditional InSAR studies can often be contaminated by potential atmospheric artifacts in SAR images and phase unwrapping errors such as DEM errors. Zebker[13] suggested that a 20% spatial or temporal change in relative humidity could result in a 10-to 14-cm error in deformation measurement retrievals. In the Agung volcano area, atmospheric artifacts were severe in certain SAR images. Figure 2 shows three unwrapped interferograms. The first interferogram was created using two images taken on July 9, 2007 and August 24, 2007. The second interferogram was produced using images taken on August 24, 2007 and October 9, 2007. The third interferogram was obtained using images taken on July 9, 2007 and October 9, 2007. As shown in the figure, the color patterns of the first two interferograms were very different from one another. Moreover, the phase difference between the cone and flank was approximately 3 - 4 radians, which was high compared to the topography. Typically, this characteristic is induced by atmospheric artifacts. Furthermore, the third interferogram did not show significant phase differences. Thus, we concluded that the large phase differences shown in figures 2(a) and 2(b) were caused by atmospheric artifacts on the image obtained on August 24, 2007.

Due to the presence of atmospheric artifacts, we used the SBAS-InSAR algorithm, which was originally proposed by Berardino[14] and refined by Jung[15]. The SBAS-InSAR algorithm is a robust InSAR time series analytical approach that uses interferograms with small baselines to minimize the effects of spatial decorrelation and topographic errors. The atmospheric artifacts were mitigated through temporal high-pass and spatial low-pass filtering of interferograms because atmospheric artifacts are highly correlated in space but poorly correlated in time[14-16]. The refined SBAS-InSAR algorithm improved the time series deformation in four ways. Namely, high-quality interferograms were used to correct phase unwrapping errors, an iteration procedure was performed to estimate the deformation and errors, the finite difference smoothing approach was used to reduce the temporal noise, and error in the reference point was corrected[15].

To select InSAR pairs for using in SBAS processing, the baselines of all possible combinations were estimated. Subsequently, we selected the InSAR combinations that exhibited a mutual perpendicular baseline less than 1000 m, and the corresponding time span intervals were set to less than 6 months. From all of the

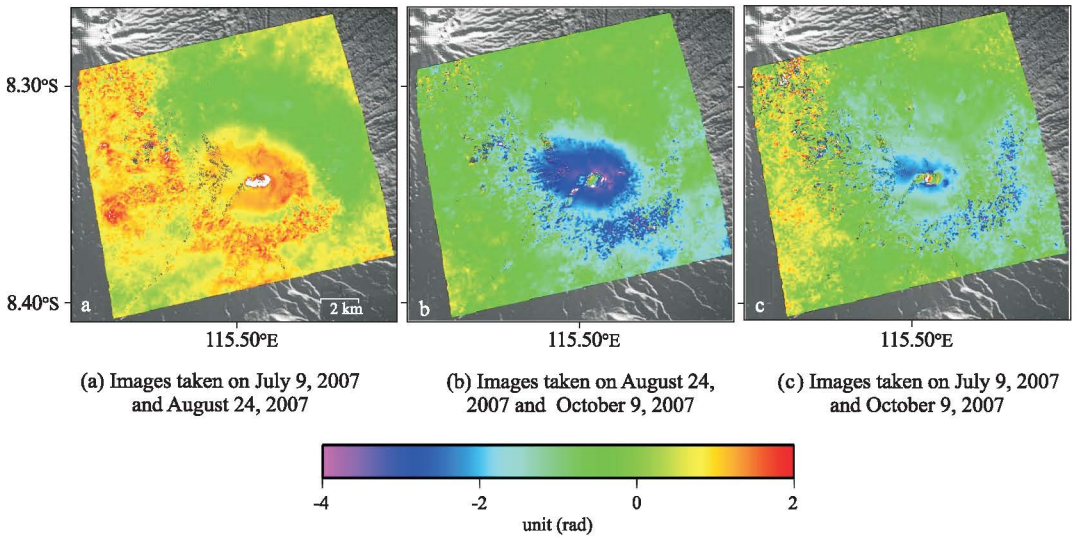

(a) Images taken on July 9, 2007 and August 24, 2007

(b) Images taken on August 24, 2007 and October 9, 2007

(c) Images taken on July 9, 2007 and October 9, 2007

Figure 2 Unwrapped interferograms showing atmospheric artifacts

interferograms, a complex multi-look operation was applied, with 4 by 9 looks in the range and azimuth, respectively. The ground range pixel dimensions of the interferograms were approximately 30 × 30 m in the range and azimuth directions. We selected 12 high signals to noise ratio interferograms, which were contained in one subset, as indicated by the connecting lines in figure 3. Prior to SBAS processing, we determined and removed baseline errors in several interferograms based on an existing DEM using a least-squares approach[17,18].

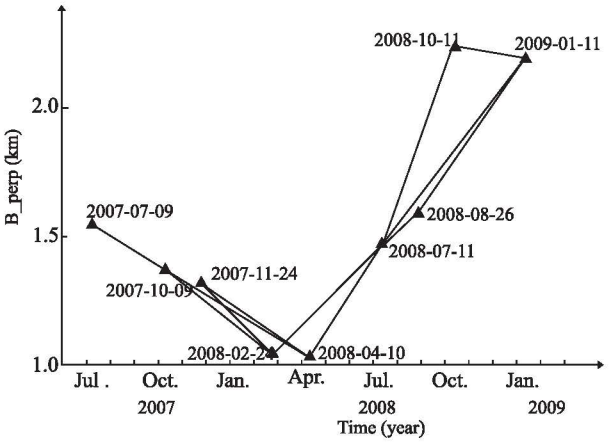

Figure 3 Baselines and InSAR combinations. Images are denoted by black triangles and labeled with the corresponding date. Black solid lines connecting triangles represent perpendicular baselines of the corresponding interferograms

2.3 SBAS-InSAR-derived time series deformation

Figure 4 shows the time series deformation fields from SBAS-InSAR. Clearly, the Agung volcano inflated between July 9, 2007 and January 11, 2009. The displacement order increased from the flank area to the top, and the largest inflating displacement was greater than 12 cm in 552 days. Figure 5 shows the time series plots for selected areas located in different parts of the volcano. The points labeled as CO and FL showed similar inflation trends, which were steady over time. The point labeled as CO was located at the western part of the cone, where displacement reached 12 cm, while the point named FL was located at the northern flank of the volcanic edifice, where displacement reached 5 cm. The displacement of the point labeled as NR was close to the reference point; thus, this point was considered to be stable.

3 Deformation modeling and analysis

Based on the shapes and radial patterns of the displacement fields, we assumed that the deformation was caused by volume changes in a spherical magma reservoir. Therefore, to interpret the magma dynamic mechanism, we modeled the time series deformation field shown in figure 4(h) with inflating point source[19] and uniformly pressured vertical prolate spheroid model[20] in an elastic half-space. In the models, we added three

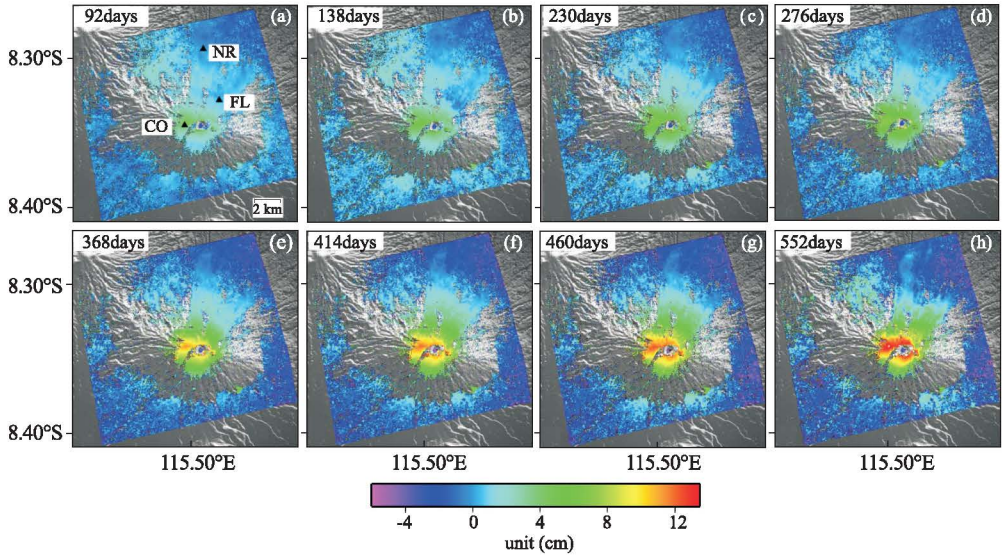

Figure 4 Time series deformation fields derived by SBAS-InSAR (LOS) in July of 2007 and January of 2009. Accumulated deformation of (a) 12 days, (b) 138 days, (c) 230 days, (d) 276 days, (e) 368 days, (f) 414 days, (e) 460 days, (h) 552 days, are shown. The uncolored areas are zones of low phase coherence that were masked during processing

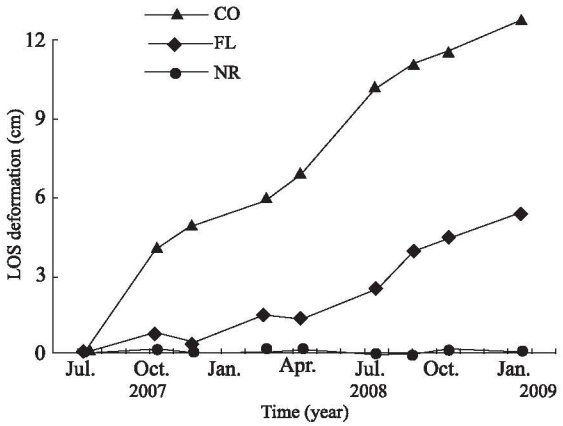

Figure 5 InSAR LOS time series deformation for the areas marked by the black triangles labeled in figure 4(a)

additional parameters, including the planar phase gradients in the x and y directions and the static shift between the model and the data. For the interferogram, we determined the best-fit parameters for the location and volume change of the deformation source. We used the downhill simplex method and Monte Carlo simulations[21] to estimate optimal parameters and uncertainties and employed the root mean square error (RMSE) between the observed and modeled interferograms as the prediction-fit criterion.

Figure 6 shows the modeling results for a Mogi point source and vertical prolate spheroid source. The modeled interferograms fit the observed interferogram reasonably well. All of the parameters were well constrained according to the uncertainties shown in table 1. The horizontal positions for the two models were similar and located around the center of the crater. However, the depth of the vertical prolate spheroid source was slightly deeper than that of the Mogi source. Subsequently, we plotted the profile across the volcanic edifice (the profile is shown in figure 6(a)). Figure 6(f) indicated that the Mogi model fit the flank area well but did not fit the top region. Moreover, the vertical prolate spheroid model fit the majority of the volcano reasonably well. Therefore, we concluded that the vertical prolate spheroid model provided the best fit.

Based on the time series deformation and modeling tests described above, the Agung volcano inflated in 2007 – 2009, and the magma chamber located at a depth of 5 km below the summit (approximately 2 km below sea level).

4 Conclusions

Fourteen InSAR images were used to map the deformation of the Agung volcano in 2007 – 2009. The deformation results showed that the Agung volcano inflated in 2007 – 2009 at a nearly constant rate. Deformation modeling tests indicated that uniformly pressured vertical

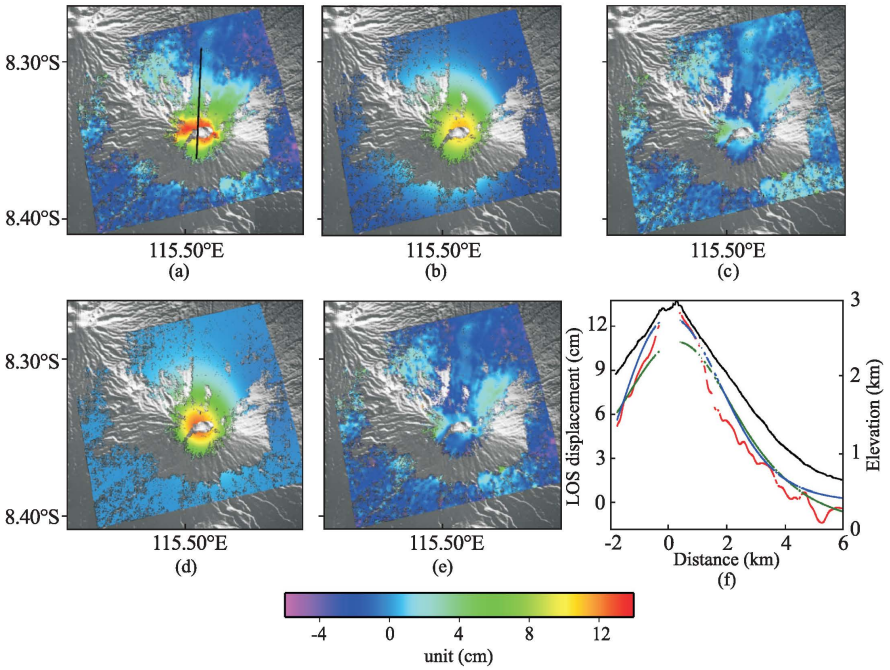

Figure 6 Results from observed and modeled deformation fields and their residual maps: (a) average filtered accumulated deformation field shown in figure 4(h); where the black line represents the position of the profile; (b) modeled deformation field from the Mogi source; (c) residual of the observed deformation (Fig. 6(a)) minus the Mogi-modeled deformation (Fig. 6(b)); (d) modeled deformation field from the vertical prolate spheroid source; (e) residual of the observed deformation field (Fig. 6(a)) minus the vertical prolate spheroid modeled-deformation (Fig. 6(d)); (f) Profiles show the observed deformation (red), modeled deformation and topography (black). The green and blue lines show the Mogi and vertical prolate spheroid modeling profiles, respectively.

Table 1 Magma chamber parameters of Agung volcano, uncertainties show 95% confidence

Parameters	Mogi	Vertical prolate spheroid
X (km)	10.5 ± 0.9	9.9 ± 1.0
Y (km)	7.7 ± 0.8	7.5 ± 1.2
Depth (km)	0.7 ± 0.8	2.1 ± 0.5
Long axis (km)	—	2.2 ± 0.7
Minor axis (km)	—	0.02 ± 0.5
Volume change (m^3)	$(3.4 \pm 1.4) \times 10^5$	$(3.0 \pm 1.0) \times 10^5$

Note: The reference for the horizontal coordinates (X, Y) was the southwestern corner of the area shown in figure 6(a).

prolate spheroid source provided a good fit for the observed volcano-wide deformation. The prolate spheroid located beneath the center of the cone at a depth of 5 km below the summit.

In the present investigation, we performed a pilot study on the potential deformation of the Agung volcano area. Our results outlined the capabilities of InSAR-based geodesy and provided a methodology for future deformation monitoring in areas that lack ground-based monitoring. Although InSAR is not a substitute for field observations, it allows researchers to more easily identify deformation areas, which can be prioritized for ground-based monitoring.

References

[1] Dilmy A. Pioneer plants found one year after the 1963 eruption of Agung in Bali. Pac. Sci., 1965,19(4): 498 - 501.

[2] Frederic E Volz. Atmospheric turbidity after the Agung eruption of 1963 and size distribution of the volcanic aerosol. J Geophys Res., 1970, 75(27): 5185 - 5194.

[3] Massonnet D, Briole P and Arnaud A. Deflation of Mount Etna monitored by spaceborne radar interferometry. Nature, 1995, 375, 567 - 570.

[4] Hooper A, Zebker H, Segall P, et al. A new method for measuring deformation on volcanoes and other natural terrains using InSAR persistent scatterers. Geophys Res Lett., 2004, 31, L23611.

[5] Hooper A, Segall P and Zebker H. Persistent scatterer InSAR for crustal deformation analysis, with application to volcano Alcedo, Galapagos. J Geophys Res., 2007, 112, B07407.

[6] Peltier A, Bianchi M, Kaminski E, et al. PSInSAR as a new tool

to monitor preeruptive volcano ground deformation: Validation using GPS measurements on Piton de la Fournaise. Geophys Res Lett., 2010, 37, L12301.

[7] Lundgren P, Casu F, Manzo M, et al. Gravity and magma induced spreading of Mount Etna volcano revealed by satellite radar interferometry. Geophys Res Lett., 2004, 31(4):L04602

[8] Pepe A, Manzo M, Casu F, et al. Surface deformation of active volcanic areas retrieved with the SBAS-DInSAR technique: an overview. Annals of Geophysics, 2008,51(1):247 -263.

[9] Casu F, Poland M P, Solaro G, et al. Surface deformation dynamics of Mauna Loa and Kilauea volcanoes, Hawaii, revealed by InSAR time series analysis. American Geophysical Union, Fall Meeting, 2008, V11B -2023.

[10] Lee C W, Lu Z, Jung H S, et al. Surface deformation of Augustine Volcano,1992 -2005,from multiple-interferogram processing using a refined Small Baseline Subset (SBAS) Interferometric Synthetic Aperture Radar (InSAR) approach. The 2006 eruption of Augustine Volcano, Alaska: U. S. Geological Survey Professional Paper 1769: 453 -465.

[11] Ji Lingyun, Wang Qingliang, Cui Duxin, et al. Time series of deformation in Tengchong volcanic area extracted by SBAS-DInSAR, Journal of Geodesy and Geodynamics, 2011, 31(4): 149 -154. (in Chinese)

[12] Philibosian B and Simons M. A survey of volcanic deformation on Java using ALOS PALSAR interferometric time series. Geochem Geophys Geosyst., 2011,12, Q11004.

[13] Zebker H A, Rosen P A and Hensley S. Atmospheric effects in interferometric synthetic aperture radar surface deformation and topographic maps. J Geophys Res., 1997, 102, 7547 -7563.

[14] Berardino P, Fornaro G, Lanari R and Sansosti E. A new algorithm for surface deformation monitoring based on small baseline differential SAR interferograms. Institute of Electrical and Electronics Engineers Transactions on Geosciences and Remote Sensing, 2002, 40(11): 2375 -2383.

[15] Jung H S, Lee C W, Park J W, Kim K D and Won J S. Improvement of small baseline subset (SBAS) algorithm for measuring time-series surface deformations from differential SAR interferograms. Korean Journal of Remote Sensing, 2008,24, 165 -177. (in Korean)

[16] Ferretti A, Prati C and Rocca F. Nonlinear subsidence rate estimation using permanent scatterers in differential SAR interferometry. IEEE Transactions on Geoscience and Remote Sensing, 2000, 38(5): 2202 -2212.

[17] Rosen P, Hensley S, Zebker H, Webb F H and Fielding E J. Surface deformation and coherence measurements of Kilauea Volcano, Hawaii, from SIR-C radar interferometry. Jour Geophys Rea., 1996, 101:23109 -23125.

[18] Lu Z. InSAR imaging of volcanic deformation over cloud-prone areas-Aleutian islands. Photog Engi Rem Sens., 2007,73(3): 245 -257.

[19] Mogi K. Relations between the eruptions of various volcanoes and the deformations of the ground surface around them. Bull Earthquake Res., Institute University. Tokyo, 1958,36: 99 -134.

[20] Yang X M, Davis P and Dieterich J H. Deformation from inflation of a dipping finite prolate spheroid in an elastic half-space as a model for volcanic stressing. J Geophys Res., 1988,93: 4249 -4257.

[21] Press W, Teukolsky S, Vetterling W and Flannery B. Numerical Recipes in C, the Art of Scientific Computing. Cambridge University. Press, New York, 1992,994.